

# THE DYNAMIC PERFORMANCE OF CAVITATING TURBOPUMPS

Christopher Brennen and Allan J. Acosta  
California Institute of Technology  
Pasadena, California, U. S. A. 91125

## Abstract

Knowledge of the dynamic performance of turbopumps is essential for the prediction of instabilities in hydraulic systems; the necessary information is in the form of a transfer function relating the instantaneous pressures and mass flow rates at inlet and discharge. Cavitation has a significant effect on this transfer function since dynamical changes in the volume of cavitation contribute to the difference in the instantaneous flow rates. The present paper synthesizes the transfer matrix for cavitating inducers at moderately low frequencies and shows that the numerical results are consistent with observations on rocket engine turbopumps.

## 1. INTRODUCTION

The advent of high performance pumps with cavitating inducers and their inclusion in increasingly complex hydraulic systems has created a definite need for improved understanding of the dynamic characteristics of such turbomachines when subjected to transient or oscillatory conditions at inlet and/or discharge. Much information, of course, exists on transient pipeline problems in hydropower systems<sup>1,2</sup>, boiler-fed systems<sup>3,4</sup> and other applications when only a single phase is involved; much less knowledge is available when a second (vapor) phase makes its appearance<sup>5,6,10</sup>. Turbomachines present more complicated problems as far as dynamical analysis is concerned though there have been some recent advances in understanding self-excited resonances<sup>5,6,7</sup>. The classical "circle" diagram of Knapp<sup>11</sup> is relevant only to very low frequencies in which the flow proceeds through a series of quasi-steady states. Even in non-cavitating operation one would expect quantities such as pump gain and resistance to be functions of some reduced frequency when this became of order one or greater. Cavitation adds another dimension since the growth and/or decrease in the volume of vapor within the pump leads to differences in the instantaneous mass flow rates into and out of the turbomachine. Linearizing the dynamics by confining attention to small oscillations about a particular steady operating point, the problem is therefore to determine the transfer function [Z] for the cavitating turbomachine where

$$\begin{Bmatrix} \tilde{p}_2 - \tilde{p}_1 \\ \tilde{m}_2 - \tilde{m}_1 \end{Bmatrix} = \begin{bmatrix} Z_{11} & Z_{12} \\ Z_{21} & Z_{22} \end{bmatrix} \begin{Bmatrix} \tilde{p}_1 \\ \tilde{m}_1 \end{Bmatrix} \quad (1)$$

$\tilde{p}_1$ ,  $\tilde{m}_1$  being the fluctuating pressure and mass flow rate at inlet and  $\tilde{p}_2$ ,  $\tilde{m}_2$  the corresponding quantities at discharge; it is convenient to regard these as dimensionless quantities related to the dimensional quantities  $\tilde{p}_{1,2}^*$ ,  $\tilde{p}_2^*$ ,  $\tilde{m}_1^*$ ,  $\tilde{m}_2^*$  by

$$\tilde{p}_{1,2} = \frac{\tilde{p}_{1,2}^*}{\frac{1}{2} \rho U_T^2} ; \quad \tilde{m}_{1,2} = \frac{\tilde{m}_{1,2}^*}{\rho A_1 U_T} \quad (2)$$

where  $U_T$  is the tip speed,  $A_1$  the inlet area and  $\rho$  the fluid density. Furthermore we define a reduced frequency,  $\omega = \Omega H / U_T$  where  $\Omega$  is the actual frequency of the oscillations and  $H$  the distance between impeller blade tips (see Fig. 1). The oscillatory quantities are also regarded as complex in the timewise imaginary unit  $j$  in order to represent the relative phases of those perturbations. The matrix elements  $Z_{11}$ , etc. are also complex, in general, and are functions not only of the mean operating state including the extent of cavitation in the turbomachine but also of the frequency,  $\omega$ .

It should be noted that [Z] as defined in (1) is probably the minimum information required; the size of the matrix could be further increased by incorporation of other independent fluctuating quantities such as the rotational speed of the impeller. Here we shall, for simplicity restrict attention to the basic matrix [Z] though elsewhere<sup>10</sup> we have considered the effects of fluctuating rotative speed.

Lack of information on the transfer function [Z] has presented a major stumbling block in the dynamic analysis of a number of modern hydraulic systems, and we illustrate this by a specific example. Virtually all liquid propelled rockets are susceptible to an instability, called the "POGO" instability<sup>13,14</sup>, which involves a closed loop interaction between the longitudinal structural modes of vibration and the dynamics of the propulsion system. This is an extreme hazard since it can lead to excessive accelerations of the payload, excessive stresses in the structure and premature shut-down of the engines. In simple terms it involves longitudinal structural vibrations which lead to pressure fluctuations in the fuel and oxidizer tanks and to pressure and mass flow rate oscillations in the feedlines. The cavitating, high performance turbopumps thus experience fluctuating inlet conditions and as a result the engines can produce an oscillating thrust which may lead to further amplification of the longitudinal structural vibration. Most of the essential elements in this system are well understood and quantifiable with the notable and important exception of the turbopumps. We cite this example because it is one situation in which detailed attempts have been made to understand and quantify various elements in the transfer matrix [Z]. Some investigations have tried to reconstruct the transfer function from observations on pump tests and flight data<sup>15,16,17,18,19</sup>. But pressure data alone and the absence of direct measurement of oscillatory mass flow rate requires all of these investigations to make certain assumptions concerning various dynamical elements in the system under investigation; hence these interpretations of the test observations and consequent results may be open to some question (see Section 6). Other attempts have been made at theoretical prediction of some of the elements of [Z]<sup>14,20,18,21,22,23</sup>. We shall see that all of these are incomplete in some respect. Finally, we mention other laboratory experiments which have involved the dynamical response of cavitating inducers but have not attempted to reconstruct the transfer function<sup>8,7</sup>.

## 2. TRANSFER MATRIX, FREQUENCY DEPENDENCE

Fortunately in many practical situations, including the POGO problem<sup>24</sup>, the reduced frequencies,  $\omega$ , are sufficiently small to suggest reasonable validity for solution of the matrix elements in series with ascending powers of  $\omega$  or  $j\omega$  so that for example

$$Z_{11} = Z_{11}^A + j\omega Z_{11}^B + \dots + O(\omega^2) \quad (3)$$

$$Z_{12} = Z_{12}^A + j\omega Z_{12}^B + \dots + O(\omega^2) \quad (4)$$

Consider now the relationship between the matrix elements as defined by (1) and the steady state operation to which they should asymptote as  $\omega$  tends to zero. Clearly then  $Z_{11}$  should tend to and  $Z_{11}^A$  should be equal to the local slope of the steady state curve of head rise against inlet pressure. Though zero under non-cavitating conditions, this element, known as the cavitating pump gain may take some non-zero value due to the influence of cavitation number on the head rise. Furthermore we may identify  $Z_{11}^B$  as a term which yields a dynamic gain different from the static pump gain. There are some indications that this may be a significant feature of turbopump dynamics<sup>19</sup>. On the other hand  $Z_{12}^A$  is recognized as the pump resistance or local slope of the steady state curve of head rise against flow rate;  $Z_{12}^B$  is clearly and inductive impedance due to the fluid inertia in the pump and is termed the pump inertance.

Unlike the elements  $Z_{11}$ ,  $Z_{12}$  the other two  $Z_{21}$ ,  $Z_{22}$  should tend to zero as  $\omega \rightarrow 0$  since the instantaneous mass flow rates should be identical in steady state operation. It follows that

$$Z_{21} = -j\omega K_B + O(\omega^2) \quad (5)$$

$$Z_{22} = -j\omega M_B + O(\omega^2) \quad (6)$$

where  $K_g$  is termed the dimensionless "compliance" of the pump and is closely related through  $K_g = C_g U_T^2 / 2HA_1$  to the dimensional compliance  $C_g$  used in space vehicle analysis<sup>20</sup>.

We call the dimensionless characteristic  $M_g$  the mass flow gain factor. Though there have been recent efforts to evaluate  $K_g$ <sup>20,22,23</sup> and to relate it to the extent and type of cavitation expected in a cavitating inducer it has been universally assumed for lack of any other knowledge to the contrary that  $Z_{22}$  and  $M_g$  were identically zero. One purpose of this paper is to demonstrate that  $M_g$  is far from zero for typical inducers and may indeed represent a major dynamic effect.

### 3. AXIAL INDUCER WITH CAVITATION

In the present paper we concentrate attention on the evaluation of the transfer function for a axial cavitating inducer in a high performance turbopump. Since cavitation in an inducer can take a number of different forms (see Refs. (23,24)), it is convenient to envisage each as contributing parts to the dynamic characteristics. Though Brennen<sup>23</sup> has shown that transient bubble cavitation can contribute substantially to compliance, most investigations<sup>20,22,23</sup> have presumed that the majority of the compliance will arise from the dynamic response of the fully developed blade cavities or vaporous wakes which form on the suction sides of the blades at lower cavitation numbers,  $\sigma_T$ , defined as

$$\sigma_T = (p_1 - p_c) / \frac{1}{2} \rho (U_T^2 + U_f^2) \quad (7)$$

where  $p_1, p_c$  are the inlet and cavity (vapor) pressure and  $U_f$  is the inlet fluid velocity. The argument here is that blade cavities, when they are formed, represent the majority of the cavity volume, though other contributions may arise from bubble cavitation in the tip clearance and backflows. Consequently Brennen and Acosta<sup>12,22</sup> developed theoretical solutions for the cavitating flow and evaluated the cavitation compliance,  $K_g$ . Briefly the method involves the neglect of radial velocities and the separate solution of the flow in a series of radial annuli as indicated in Fig. 1. Each radial station is then unrolled into a cascade and the flow solved as a function of local angle of attack  $\alpha(r)$ , blade  $\beta(r)$ , blade thickness ratio  $d(r)$  and local cavitation number  $\sigma_L$  defined by

$$\sigma_L = (p_1 - p_c) / \frac{1}{2} \rho (U_B^2 + U_f^2) \quad (8)$$

where  $U_B(r)$  is the local blade velocity.

Usually  $U_f \ll U_T$  and thus  $\sigma_L$  and the overall cavitation number  $\sigma_T$  are approximately related by  $\sigma_T = R^2 \sigma_L / r^2$ . Moreover the angle of attack  $\alpha(r)$  is related to the overall flow coefficient,  $\varphi = U_f / U_T$  by

$$\alpha(r) = \frac{\pi}{2} - \beta(r) - \tan^{-1}(R\varphi/r) \quad (9)$$

A linearized cavitating cascade theory was employed to obtain flow solutions which enabled the cross-sectional area of the cavity  $A^*(r)$  to be obtained as a function of  $\alpha, \beta, d$  and  $\sigma_L$ . Defining a non-dimensional area  $a = A^*/(h(r))^2$  it follows that for a given inducer geometry the total volume of cavity in the inducer,  $V$ , which is a function of the operating conditions  $\varphi, \sigma_T$  can then be obtained by integration

$$V(\varphi, \sigma_T) = \int_{R_H}^R a(r, \sigma_L, \varphi) (h(r))^2 N dr \quad (10)$$

where  $N$  is the number of blades ( $h(r) = 2\pi r/N$ ).

### 4. COMPLIANCE, MASS FLOW GAIN FACTOR

Since the instantaneous difference between the inlet and discharge mass flow rates must be equal to the rate of change of cavity volume with time we now observe that the dynamic elements  $Z_{21}, Z_{22}$  can be evaluated from a series of quasisteady cavitating cascade solutions using the relations

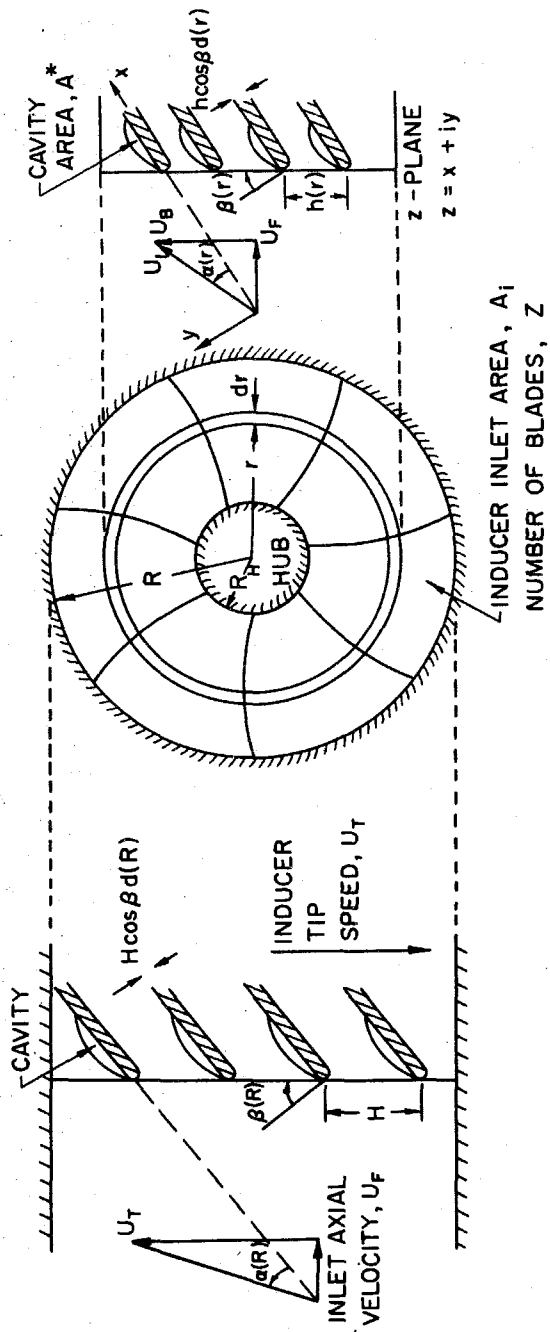


Figure 1. Inducer inlet with nomenclature.

$$Z_{21} = \frac{U_f}{2A_1} \left( \frac{\Delta(\tilde{m}_1^* - \tilde{m}_2^*)}{\Delta \tilde{p}_1^*} \right)_{\varphi = \text{const}} = j \frac{\Omega \varphi U_f}{2A_1} \left( \frac{\partial V}{\partial p_1} \right)_{\varphi = \text{const}} \quad (11)$$

$$Z_{22} = \left( \frac{\Delta(\tilde{m}_1^* - \tilde{m}_2^*)}{\Delta \tilde{m}_1^*} \right)_{\tilde{p}_1^* = 0} = j \frac{\Omega}{A_1} \left( \frac{\partial V}{\partial U_f} \right)_{\tilde{p}_1^* = 0} \quad (12)$$

These can be derived from the above observation and the definitions (1), (2). It follows from (11) that the compliance  $K_b$  given by  $Z_{21} = -j\omega K_b$  arises from changes in the cavity volume as the inlet pressure varies while the angle of attack and/or flow coefficient,  $\varphi$ , remain constant. Since usually  $U_f \gg U_r$ , the variation in inlet pressure implies variation in the cavitation number and the derivative in (11) which determines  $Z_{21}$  is essentially the change of volume with cavitation number. On the other hand the mass flow gain factor defined by  $Z_{22} = -j\omega M_b$  arises from volume changes with angle of attack or flow coefficient while the inlet pressure remains constant. Substituting for  $V$  from Eq. (10) and utilizing the geometric relations between  $U_f$ ,  $U_b$ ,  $\alpha$ ,  $\beta$  one obtains  $K_b$ ,  $M_b$  as

$$K_b(\varphi, \sigma_r) = \frac{2}{[1 - (R_u/R)^2]} \int_{\frac{R_u}{R}}^1 K_L(\varphi, \sigma_r, r/R) d(r/R) \quad (13)$$

$$M_b(\varphi, \sigma_r) = \frac{2}{[1 - (R_u/R)^2]} \int_{\frac{R_u}{R}}^1 M_L(\varphi, \sigma_r, r/R) (r/R) d(r/R) \quad (14)$$

where  $K_L, M_L$  are local compliances and local mass flow gain factors at each radial position given by

$$K_L = - \frac{\partial a}{\partial \sigma_L} \quad (15)$$

$$M_L = \sin(\alpha + \beta) \left[ 2\sigma_L \cos(\alpha + \beta) \frac{\partial a}{\partial \sigma_L} + \sin(\alpha + \beta) \frac{\partial a}{\partial \alpha} \right] \quad (16)$$

Thus in order to evaluate the compliance and mass flow gain factor and hence  $Z_{21}, Z_{22}$  we need only evaluate the quantities  $\partial a / \partial \sigma_L$  and  $\partial a / \partial \alpha$  for each radial position from the appropriate cascade analysis and then integrate these according to the relations (13), (14). It is worth anticipating typical numerical results to note that the term in  $M_L$  involving  $\partial a / \partial \sigma_L$  is usually small since  $\alpha + \beta$  is generally close to  $\pi/2$ ; hence

$$M_L \approx \partial a / \partial \alpha \quad (17)$$

Note that this implies the following approximate relation which can be most useful in interpreting the numerical results

$$\left( \frac{\partial M_b}{\partial \sigma_r} \right)_{\varphi = \text{const}} \approx \left( \frac{\partial K_b}{\partial \varphi} \right)_{\sigma_r = \text{const}} \quad (18)$$

That is to say the rate of change of the compliance with flow coefficient is equal to the rate of change of mass flow gain factor with cavitation number.

Furthermore observe that the choice in definition of  $K_L, M_L$  implies through the relation (13), (14) that if  $K_L$  increases linearly with radial position and  $M_L$  is independent of  $r$  then  $K_b, M_b$  are simply equal to the values of  $K_L, M_L$  at the blade tip. Frequently these are useful first approximations.

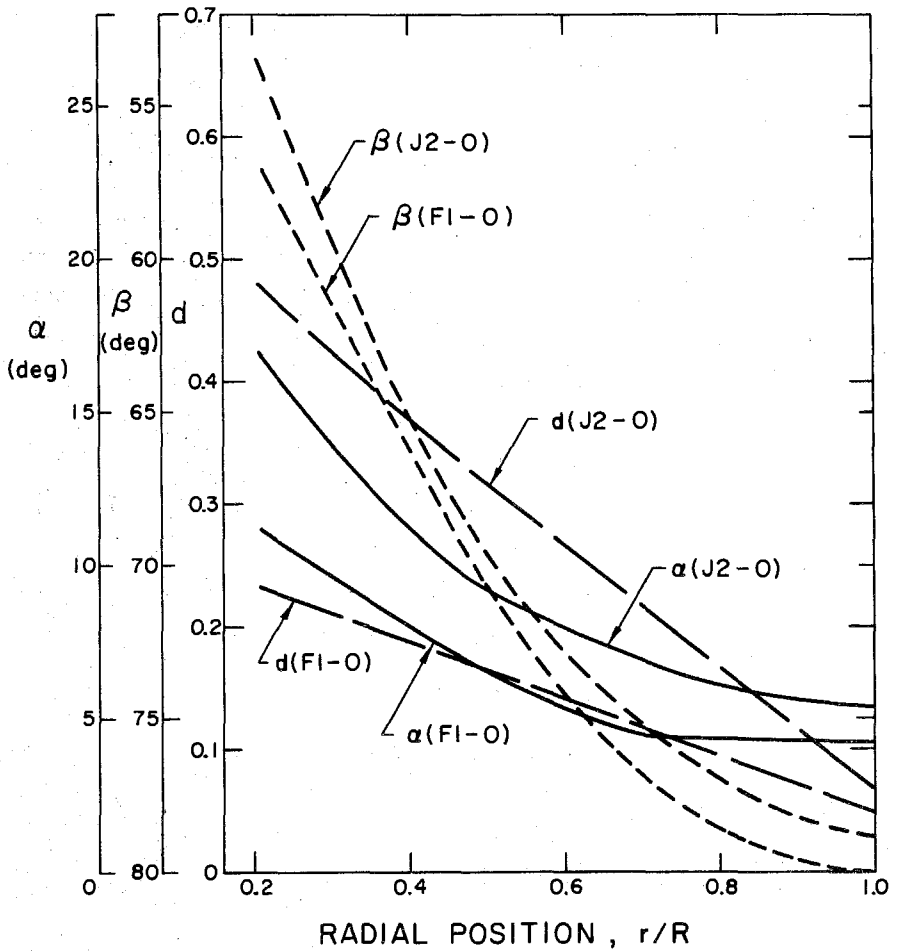


Figure 2. Radial variations of the blade angle,  $\beta$ , blade thickness to normal spacing ratio,  $d$ , and angle of attack  $\alpha$  (for  $\phi = 0.097$ ) for the oxidizer turbopump inducers in the Saturn J1 and F1 engines.

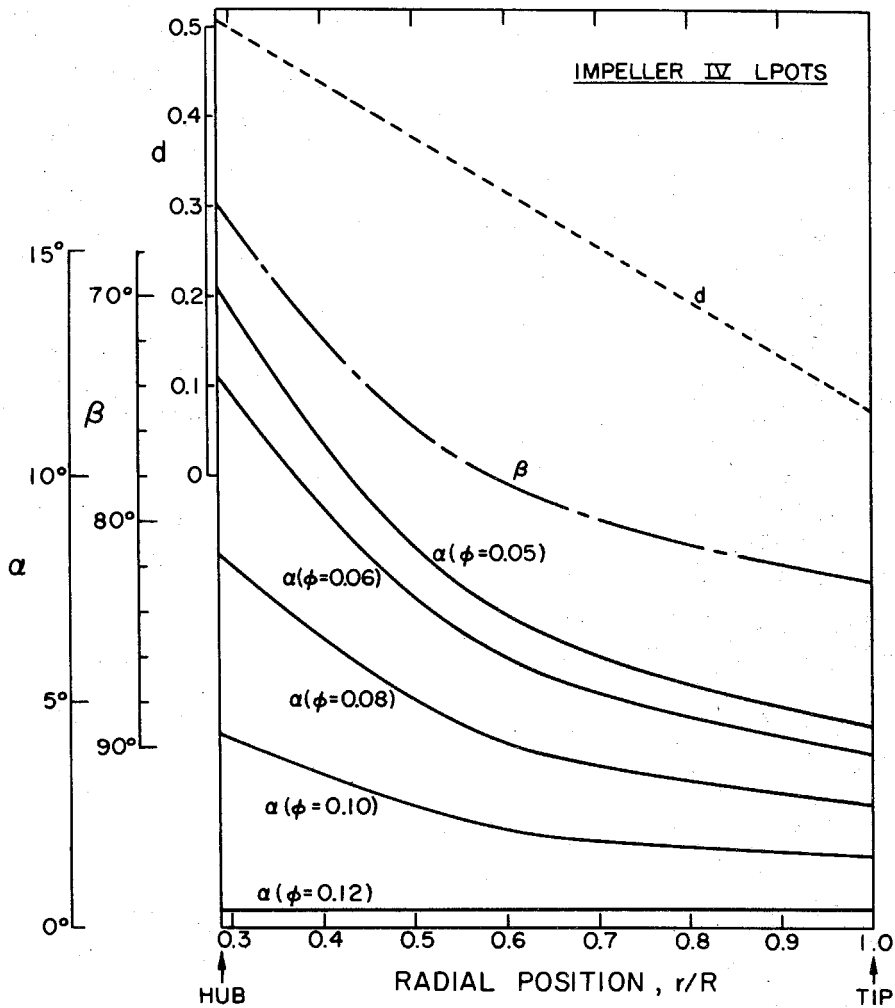


Figure 3. Radial variations of the blade angle,  $\beta$ , blade thickness to normal spacing ratio,  $d$ , and angle of attack,  $\alpha$ , (for various flow coefficients,  $\phi$ ) for the low pressure oxidizer turbopump of the main Shuttle engine (designated Impeller IV LPOTS).

## 5. APPLICATION TO TURBOPUMPS

With the ability to evaluate the compliance and mass flow gain factor we are now in the position of being able to obtain the first non-zero terms in the expansions of all of the elements  $Z_{11}, Z_{12}, Z_{21}, Z_{22}$  in the transfer function. This should allow first order or low frequency analysis of dynamic turbopump characteristics and we shall illustrate this by application to liquid propelled rocket turbopumps. Figures 2 and 3 illustrate the necessary initial information on inducer geometry, namely blade angle and blade thickness as a function of radial position; Fig. 2 is relevant to the oxidizer pump (J2-0) on the J2 Saturn engine while Fig. 3 presents data on the proposed low pressure oxidizer pump for the main engines of the Shuttle Space vehicle. Though data has also been obtained for other fuel and oxidizer turbopumps we shall confine ourselves here to these two examples. The first is chosen because of the extensive dynamic tests which have been performed on it<sup>16,17,18</sup>, and the resulting comparison which can be made with the theory (see next Section); the latter is chosen because of its current interest.

By way of example, the resulting radial distributions of local compliance,  $K_L$ , and local mass flow gain factor,  $M_L$ , for the Shuttle inducer are shown in Fig. 4. Integrated total compliances,  $K_B$ , and mass flow gain factors,  $M_B$ , are included in Figs. 5 and 6. Perhaps the most significant feature of the results is that, over most of the range of cavitation number the mass flow gain factor  $M_B$  is significantly larger than the compliance,  $K_B$ . This strongly suggests that any dynamic transfer function which omits  $Z_{22}$  while retaining  $Z_{21}$  could be seriously in error.

## 6. COMPARISON WITH TEST OBSERVATIONS ON SATURN ENGINE

Since extensive dynamic tests were performed on the Saturn J2 engine, we shall use this data for a comparison between the theory and test observations. Lumped parameter electrical analogies are commonly employed to model the experimental observations. The simplest turbopump model used, for example, by Murphy<sup>15</sup> consists of a compliance element, C, a pressure (voltage) amplifier, G, representing the pump gain and a pump resistance, R (Model A. Fig. 7). The discharge line is represented by an inductance, L, and a discharge resistance,  $R_D$ . However in the tests considered here  $R_D$  was estimated to be small compared with R (Ref. 15 and private communication) so for convenience we shall assume that it is absorbed in R and that the load is purely inductive.

The experimental observations which consist of pressure fluctuation measurements only over a range of perturbation frequencies,  $\Omega$ , are commonly analyzed in the following way. First theoretical estimates are made for some of the quantities such as L, R, and G, the last being close to unity. Then the observations are analyzed to find the compliance, C, at various cavitation numbers which yields the best fit to the input impedance of the electrical analogy. One of the most detailed investigations of this type was that performed on the J2 oxidizer turbopump<sup>18,17,19</sup>. However it became apparent in those tests that a single compliance, C, was insufficient to properly match the dynamic data and a modification, known as the "double-compliance model" (Model B, Fig. 7) was suggested since it appeared more consistent with the observations. The input impedance of this model is

$$\frac{\tilde{p}_1^*}{\tilde{m}_1^*} = \frac{R + j\Omega(L + RR_2C_2) - \Omega^2 LC_2 R_2}{G + j\Omega(CR + GC_2 R_2) - \Omega^2(LC + RCR_2 C_2) - j\Omega^3 LCR_2 C_2} \quad (19)$$

and values of C,  $R_1/G$ ,  $R_2/G$ ,  $GC_2$  and  $L/G$  deduced from the tests on the J2-0 turbopump are given by Vaager, Fidler and Zehnle<sup>18</sup>. The same dimensional values of the compliance, C, and  $R/G$  are listed in Table 1; furthermore the compliance, C, is plotted in Fig. 6.

In the past such compliances were directly compared with the theoretical values<sup>2,2</sup>; as illustrated in Fig. 6 this led to the perplexing conclusion that the theoretical values were some three to ten times smaller than the "observed" values<sup>2,2</sup>. We shall now demonstrate that such comparisons were inappropriate.



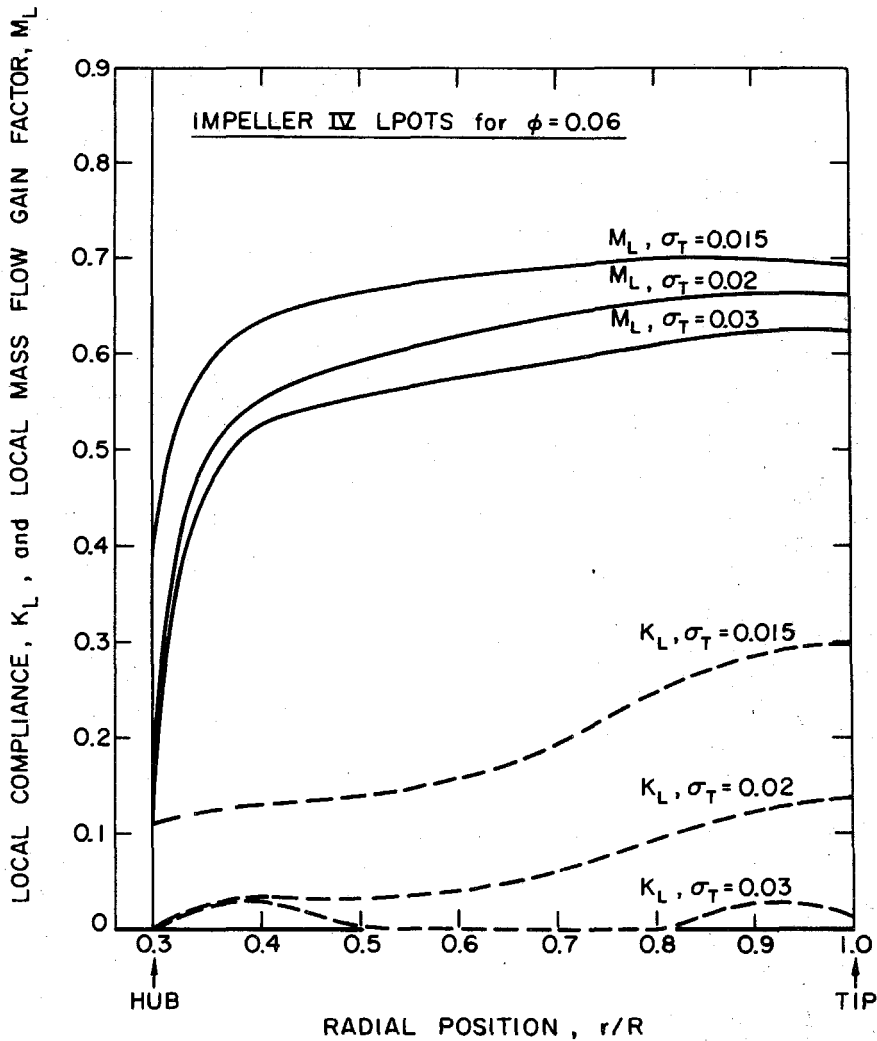


Figure 4. Example of the radial distributions of compliance,  $K_L$ , and mass flow gain factor,  $M_L$ , for Impeller IV LPOTS at a flow coefficient of 0.06 and various tip cavitation numbers,  $\sigma_T$ .

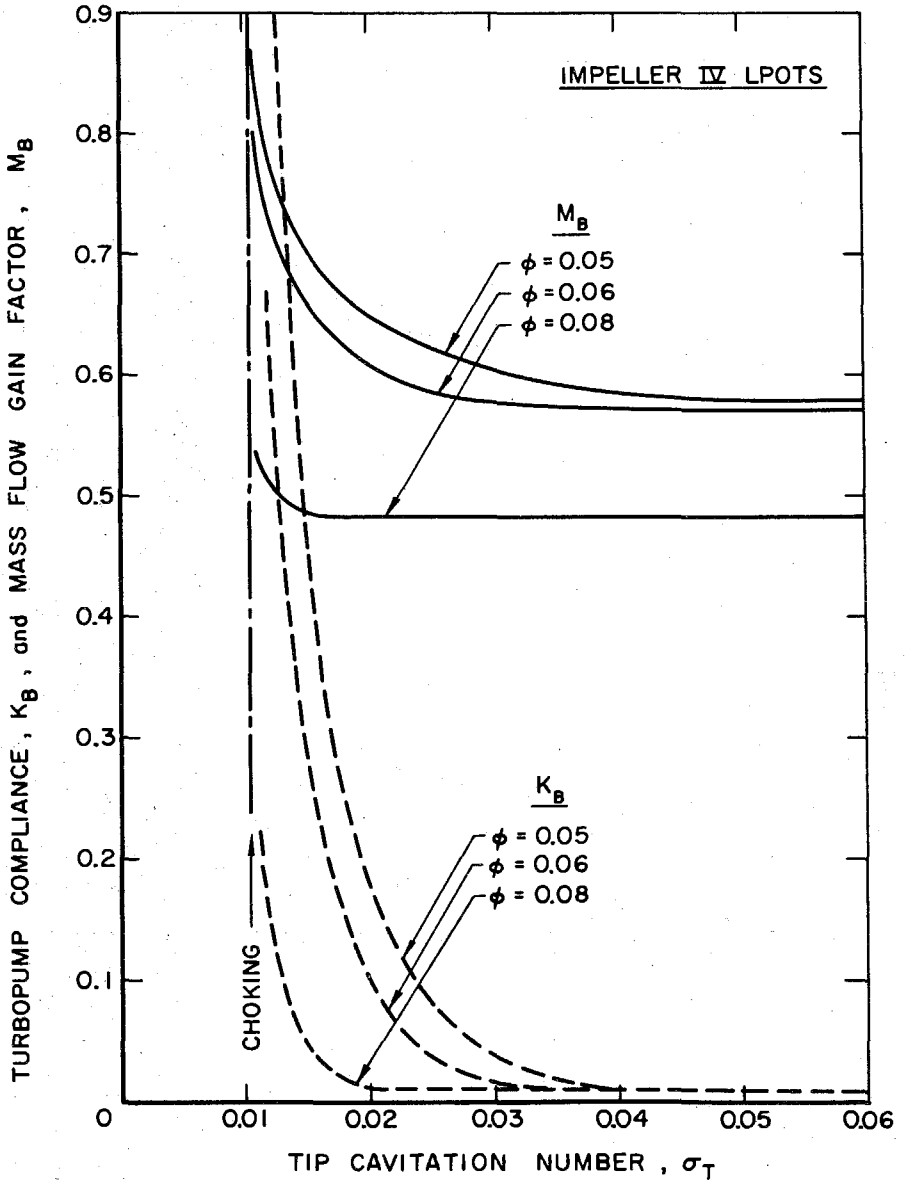


Figure 5. Calculated compliance,  $K_B$ , and mass flow gain factor,  $M_B$ , for low pressure oxidizer turbopump in the main Shuttle engine (Impeller IV LPOTS) as a function of flow coefficient and tip cavitation number,  $\sigma_T$ .

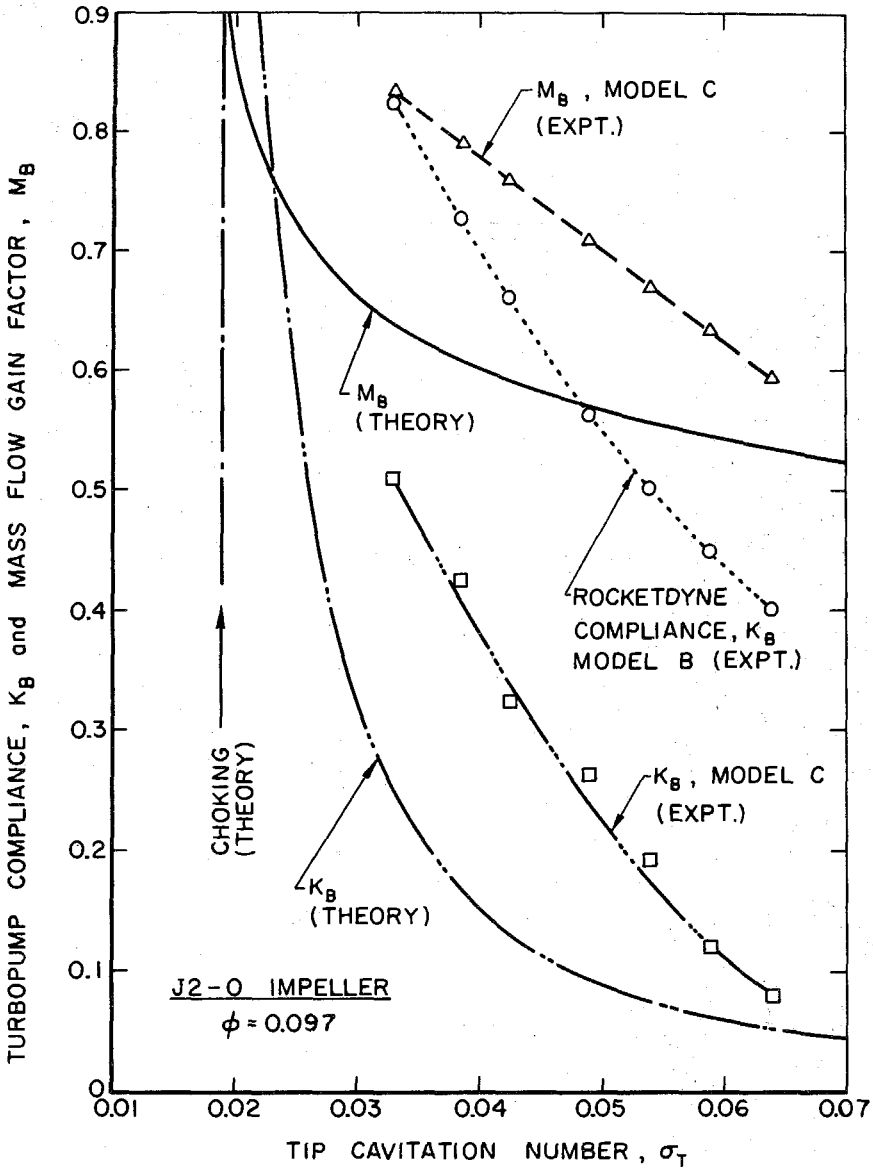


Figure 6. Dynamic characteristics of the J2-0 turbopump. Theoretically calculated compliance,  $K_B$ , -----, and mass flow gain factor,  $M_B$ , ———, for  $\phi = 0.097$ . Values derived from experimental observation: (1) Main compliance, C, derived from Rocketdyne Model B, O.....O (2) Compliance,  $K_B$ , □.....□ and mass flow gain factor,  $M_B$ , Δ.....Δ, from Model C of this paper.

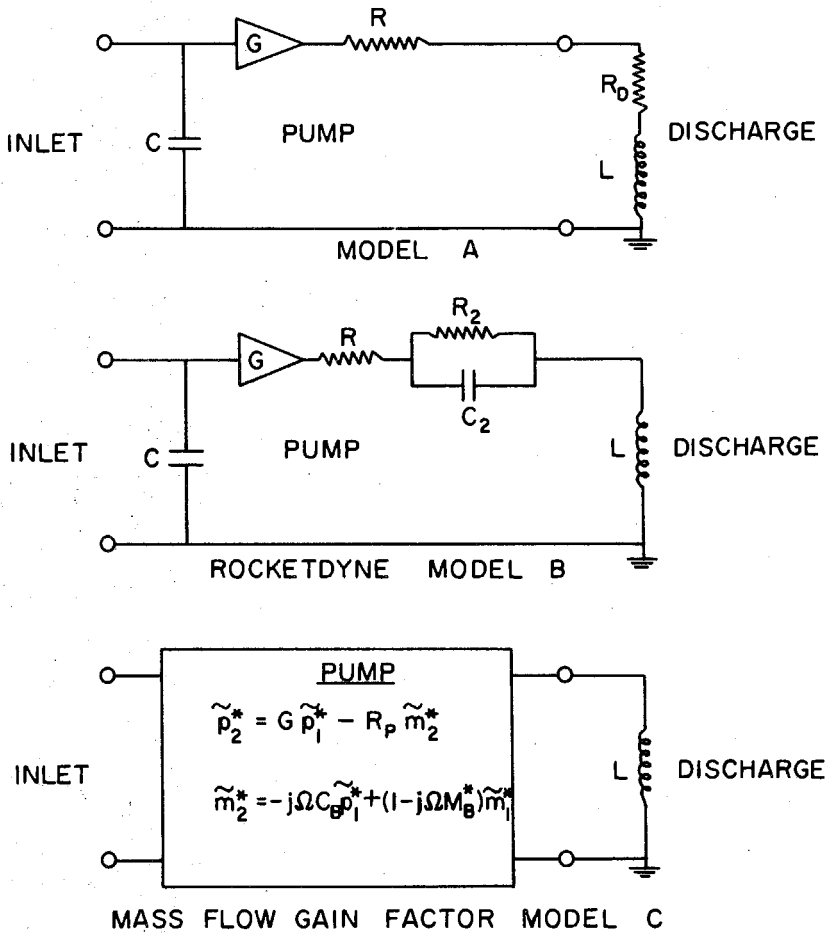


Figure 7. Electronic analogies for the dynamic behavior of cavitating turbopumps and the mass flow gain factor Model C of this paper.

First we must observe that Models A and B, Fig. 7 are purely empirical in nature and that the "compliance" used within them is not necessarily identical to the compliance more precisely defined in this paper through Eqs. (1) and (5). Indeed the considerations of this paper suggest the Model C, Fig. 7 which consists of a gain  $G$ , a resistance  $R_p$ , a dimensional compliance  $C_B$  and a dimensional mass flow gain factor  $M_B^*$  contained within a pump transfer function. The input impedance is then

$$\frac{\tilde{P}_1^*}{\tilde{m}_1^*} = \frac{R_p + j\Omega(L - M_B^* R_p) + \Omega^2 M_B^* L}{G + j\Omega C_B R_p - \Omega^2 L C_B} \quad (20)$$

Now we shall compare (19) and (20) and, using the data of Table 1, attempt to deduce actual values for the compliance,  $C_B$ , and mass flow gain factor,  $M_B^*$  relevant to the experimental observations. In doing so it is well to remember the limitations of our low frequency analysis; if (19) and (20) are equated and the result arranged as an ascending polynomial in  $j\Omega$  then we are only justified in equating to zero the coefficients of the first two terms. The first gives simply  $R_p = R$ ; the second yields the relation

$$C - C_B = \frac{M_B^* G}{R} \quad (21)$$

This relation makes clear why the "compliance",  $C$ , derived by the experimenters can be so different from the values of,  $C_B$ , derived theoretically. Essentially it is due to the total neglect of the possibility of a mass flow gain factor within the lumped parameter analogies used in analysis of the test observations; only when  $M_B^* = 0$  can  $C = C_B$ . Though the present analysis of observations cannot permit separation of  $C_B$  and  $M_B^*$  we have chosen a set of values of  $C_B$  and  $M_B^*$  which are consistent with the values of  $C$  and  $R/G$  through the relation (21); these are tabulated in Table 1 and also plotted in Fig. 6. It is clear from this figure that these estimated experimental values of compliance,  $K_B$ , and mass flow gain factor,  $M_B^*$ , are in much better agreement with theory than would be obtained had we simplistically and incorrectly compared the compliance from the Rocketdyne model with the theoretical,  $K_B$ . Indeed given the approximate nature of the experimental data the agreement is most encouraging. The somewhat greater experimental values of compliance and mass flow gain factor could arise through contributions from tip vortex, backflow and bubble cavitation volumes which are not included in the present analysis.

## 7. CONCLUDING REMARKS

It has been demonstrated that a dynamic transfer function which includes not only a compliance but also a mass flow gain factor is a satisfactory first approximation for a cavitating turbopump. In the past, neglect of the latter factor led to large discrepancies between theoretical predictions of compliance and values estimated from experimental observations. When the latter are analyzed with prior knowledge of the existence of a mass flow gain factor then the differences between theory and experiment are very much smaller and the comparison provides support for the validity of the theoretical model. The remaining differences may be ascribed to the fact that we have considered only blade cavities and have neglected additional volumes associated with tip clearance, backflow and bubble cavitation.

However there also remain limitations in the present theory. In the first place it is limited to low reduced frequencies. Furthermore we have evaluated only the first non-zero term in the expansions for each of the elements of the transfer function. A more sophisticated hydrodynamic solution is necessary in order to evaluate the second terms. Such solutions are becoming available<sup>25,26</sup> but have not as yet been incorporated in the transfer function.

Since there are indications of significant differences between the dynamic and static pump gain<sup>19</sup> it would seem that these extensions of the present model and the evaluation of  $Z_{11}^*$  in particular could be most useful and instructive.

Clearly, however, there is a dire need for more specific and detailed experimental data on the complete transfer function. Such experiments, unlike the previous

tests, should measure directly the fluctuating pressures and mass flow rates at inlet and discharge and thus permit more conclusive comparison between theory and experiment. We are presently involved in such an experiment and hope to present results in the near future.

#### ACKNOWLEDGMENT

The authors are indebted to the George Marshall Space Flight Center, Huntsville, Alabama for support under NASA Contract NAS 8-28046 and to Mr. L. Gross of NASA, Huntsville, Dr. S. Rubin of Aerospace Corporation and Dr. J. Fenwick of the Rocketdyne Division of Rockwell International for valuable suggestions and advice.

#### REFERENCES

1. Jaeger, C., "The theory of resonance in hydro-power systems, discussion of incidents and accidents occurring in pressure systems". J. Basic Eng., Vol. 85, 1963, pp. 631-640.
2. Streeter, V. L. and Wylie, E. B., "Waterhammer and surge control". Ann. Rev. Fluid Mech., Vol. 6, 1974, pp. 57-73.
3. Liao, G. S., "Protection of boiler feed pump against transient suction decay". J. Eng. for Power, Vol. 96, 1974, pp. 247-255.
4. Liao, G. S. and Leung, P., "Analysis of feedwater pump suction pressure decay under instant turbine load rejection". J. Eng. for Power, Vol. 34, 1972, pp. 83-90.
5. Zielke, W. and Hack, H. P., "Resonance frequencies and associated mode shapes of pressurized piping systems". Int. Conf. Pressure Surges, Paper G-1, Brit. Hydromech. Res. Assoc., Cranfield, England, G1-1-13, 1972.
6. Sack, L. E. and Nottage, H. B., "System oscillations associated with cavitating inducers". J. Basic Eng., Vol. 87, Series D, No. 4, 1965, pp. 917-925.
7. Natanzon, M. S., Bal'tsev, N. I., Bazhanov, V. V. and Leydervarger, M. R., "Experimental investigation of cavitation-induced oscillations of helical inducers". Fluid Mech. -Soviet Research, Vol. 3, 1974, pp. 38-45.
8. Wijngaarden, L. van, "On the equations of motion for mixtures of liquid and gas bubbles". J. Fluid Mech., Vol. 33, 1968, p. 465.
9. Weyler, M. E., Streeter, V. L. and Larsen, P. S., "An investigation of the effect of cavitation bubbles on the momentum loss in transient pipe flow". J. Fluids Eng., Vol. 93, 1971, pp. 1-10.
10. Safwat, H. H. and Van Den Polder, J., "Experimental and analytical data correlation study of water column separation". J. Fluids Eng., Vol. 95, 1973, pp. 91-97.
11. Knapp, R. T., "Complete characteristics of centrifugal pumps and their use in the prediction of transient behavior". Trans. ASME, Nov. 1937, pp. 683-689.
12. Brennen, C. and Acosta, A. J. "The dynamic transfer function for a cavitating inducer. Submitted to J. Fluids Eng., 1975.
13. Prevention of coupled-structure propulsion instability (POGO), NASA SP-8055, Oct. 1970.
14. Rubin, S., "Longitudinal instability of liquid rockets due to propulsion feedback (POGO)". J. Spacecraft and Rockets, Vol. 3, No. 8, 1966, pp. 1188-1195.
15. Murphy, G. L., "Pogo suppression analysis of the S-II and S-IVB LOX feed systems". Summary Report ASD-ASTN-1040, Brown Engineering Co., Huntsville, Alabama, 1969.
16. Rocketdyne Report, "J-2 Vehicle longitudinal stability (POGO) analysis program". Rocketdyne Division, North American Rockwell, Report No. R-6283, Aug. 1965.
17. Rocketdyne Report, "Investigation of 17-Hz, closed-loop instability on S-II stage of Saturn V". Rocketdyne Division, North American Rockwell, Report No. R-7970, Aug. 1969.

18. Vaage, R. D., Fidler, L. E. and Zehnle, R. A., "Investigation of characteristics of feed system instabilities". Final Report MCR-72-107, Martin Marietta Corporation, Denver, Colo., May 1972.
19. Wagner, R. G., "Titan II engine transfer function test results". Report No. TOR-0059(6471)-9, Aerospace Corporation, El Segundo, Calif., Feb. 1971.
20. Ghahremani, F. G. and Rubin, S., "Empirical evaluation of pump inlet compliance". Final Report No. ATR-73(7257)-1, Aerospace Corporation, El Segundo, Calif., July 1972.
21. Kim, J. H. and Acosta, A. J., "Unsteady flow in cavitating turbopumps". J. Fluids Eng., Vol. 96, 1974, pp. 25-28.
22. Brennen, C. and Acosta, A. J., "Theoretical, quasi-static analysis of cavitation compliance in turbopumps". J. Spacecraft and Rockets, Vol. 10, No. 3, 1973, pp. 175-180.
23. Brennen, C., "The dynamic behavior and compliance of a stream of cavitating bubbles". J. Fluids Eng., Vol. 95, Series 1, No. 4, 1973, pp. 533-542.
24. Lakshminarayana, B., "Three dimensional flow field in rocket pump inducers. Part 1: Measured flow field inside the rotating blade passage and at the exit". J. Fluids Eng., Vol. 95, 1973, pp. 567-578.

TABLE 1

Numerical values for the J2-0 turbopump according to the Model B, Fig. 7 from Vaage, Fidler and Zehnle (1971) and equivalent values of  $C_B$  and  $M_B^*$  for the mass flow gain factor Model C.

TIP CAVITATION NUMBER	ROCKETDYNE MODEL B		* MASS FLOW GAIN FACTOR MODEL C	
	C ( $m^2 \times 10^6$ )	R/G ( $m^{-2}s \times 10^{-3}$ )	$C_B$ ( $m^2 \times 10^6$ )	$M_B^*$ ( $s \times 10^2$ )
0.0330	1.22	0.65	0.76	0.30
0.0385	1.13	0.57	0.64	0.28
0.0425	0.91	0.58	0.48	0.27
0.0490	0.86	0.54	0.41	0.25
0.0540	0.79	0.49	0.30	0.24
0.0590	0.66	0.47	0.17	0.23
0.0635	0.52	0.51	0.11	0.21

\* For the J2-0 pump the non-dimensional  $K_B$  is given by  $C_B / (1.48 \times 10^{-6} m^2)$  for the non-dimensional  $M_B$  by  $M_B^* \times (279 s^{-1})$ .